

## Optical index gratings in electromagnetically aligned shaped-microparticle suspensions

D. Rogovin and J. Scholl

*Rockwell Science Center, Thousand Oaks, California 91360*

(Received 7 December 1990)

We study the nonlinear optical response of an electromagnetically aligned shaped-microparticle suspension, and focus on the physical characteristics of static, microparticle index gratings. Theory suggests that the physical properties of shaped-microparticle index gratings can be considerably altered by aligning the suspension with either an electric field or polarized radiation. Specifically, the medium response times are reduced, the grating polarization characteristics are altered, and depending upon the specific situation, the index grating depth can be either increased or decreased.

### I. INTRODUCTION

The nonlinear optics of microparticle suspensions and aerosols is of considerable interest to the physics and laser communities. Early studies centered on spherical microparticles,<sup>1-3</sup> in which nonlinear optical effects arise from particle translation. More recent studies examined shaped-microparticle suspensions<sup>4-16</sup> wherein nonlinear optical effects arise from both particle translation and rotation. Attention has focused on the nonlinear electrodynamic response of shaped-microparticle suspensions to coherent radiation at visible, microwave, and millimeter wavelengths. Optical birefringence,<sup>4-7</sup> electric-field birefringence,<sup>8,9</sup> optical phase conjugation via degenerate<sup>10-12</sup> four-wave mixing (DFWM), as well as coherent beam combination<sup>13</sup> via nondegenerate two-wave mixing have been successfully demonstrated in this class of active optical media.

The nonlinear optical response of shaped-microparticle suspensions is based on radiation-induced, electrostrictive forces and torques that translate and rotate the microparticles into certain specified positions and orientations.<sup>4-16</sup> This motion alters the suspension's dielectric constant, which gives rise to the nonlinear phenomena noted above. Since microparticle orientation is the basis for the nonlinear optical processes that these media exhibit, it is logical to examine the consequences of placing the suspension in a highly oriented, anisotropic state. This can be attained with a strong electric field, an intense polarized radiation beam, acoustic waves, laminar flow, or even by chemical means. Theory suggests that such orienting fields will vastly alter the nonlinear optical properties and transient dynamics of microparticle suspensions.<sup>16</sup> Furthermore, there exists experimental data that supports this notion.<sup>17</sup>

This paper examines the physical properties of static optical index gratings in electromagnetically aligned shaped-microparticle suspensions and contrasts them with index gratings created in unaligned suspensions. We focus on situations in which the microparticles are aligned by means of either an electric field or by a single, linearly polarized radiation beam.<sup>18</sup> The field that aligns the particles is referred to as the orienting field. Other schemes for achieving an aligned medium will be dis-

cussed elsewhere. Although the theory is formulated for shaped-microparticle suspensions, much of it applies to other active optical media that exhibit nonlinear phenomena mediated via orientational gratings.

We assume a monodisperse suspension of shaped microparticles characterized by an equilibrium density  $n_0$  and a frequency-dependent electromagnetic polarizability tensor  $\vec{\alpha}$ . The steady-state and transient optical properties of shaped-microparticle index gratings in unaligned suspensions are understood from prior experimental<sup>10-12</sup> and theoretical studies<sup>14,15</sup> of optical phase conjugation via degenerate four-wave mixing. Here the theoretical studies are extended to the optical and dynamical characteristics of static-microparticle index gratings in electromagnetically aligned microparticle suspensions. Grating strength and polarization characteristics, as well as grating formation and decay times are determined.

In all cases, we find that the response times of highly oriented shaped-microparticle suspensions are faster than those of isotropic ones. This interesting and potentially useful property arises from and reflects the fact that an aligning field will tend to restrict the microparticles to point within a relatively narrow range of angles. This restriction ensures that during grating formation, the microparticles need to rotate through a smaller range of angles than they do in an isotropic suspension. Accordingly, a sufficiently intense electric field or polarized radiation beam will reduce the grating formation and decay times in shaped-microparticle suspensions.

The steady-state properties of microparticle index gratings in oriented suspensions are found to differ markedly from those generated in isotropic suspensions. In an isotropic suspension, static microparticle index gratings consist of periodic, alternating regions in which the particles are aligned and then unaligned. The degree and direction of particle alignment is fixed by the incident write beams. In an electromagnetically aligned suspension, all of the microparticles tend to point in a direction specified by the aligning field and superimposed on this is the microparticle index grating that now consists of a periodic tightening and easing of the microparticle orientation about the preferred angle. Also, the properties of index gratings in an electromagnetically aligned microparticle suspension are found to depend upon whether the particles are rod shaped or disc shaped, a feature that

is not true if the particles are unaligned. The polarization characteristics of these index gratings are also altered by electromagnetic alignment. Furthermore, new types of microparticle index gratings appear if the distribution is anisotropic. These gratings exhibit mixed characteristics that are partially translational and partially orientational in nature.

Associated with these changes in the properties of microparticle index gratings are dramatic changes in the characteristics of the phase-conjugate radiation generated via DFWM. For example, the additional gratings that arise due to the anisotropic microparticle distribution can be in or out of phase with respect to the original orientational gratings. If they are out of phase, then the phase-conjugate radiation produced by these gratings will partially cancel that generated by the original gratings, resulting in smaller four-wave mixing coefficients and lower reflectivities. If the new gratings are in phase with the original ones, the four-wave mixing coefficient will be larger and the process will be more efficient. The phase relationship between these gratings depends intimately upon the orientation of the aligning field and the polarization characteristics of the write beams.

This paper is divided into four parts, of which this Introduction is first. In Sec. II, we formulate the problem of the interaction of electromagnetic radiation with shaped particles that are maintained in an orienting field. The steady-state and transient optical characteristics of electromagnetically aligned static-particle index gratings are discussed in Sec. III. Finally, in Sec. IV we summarize our results and present our conclusions on the nature of static, index gratings in electromagnetically aligned, shaped-particle suspensions. The implications of this work with respect to other types of anisotropic nonlinear media that generate phase-conjugate radiation via orientational index gratings is also discussed. A forthcoming

paper will deal with optical phase conjugation via degenerate four-wave mixing in electromagnetically aligned, shaped-microparticle suspensions.

Finally, the material in this paper is most relevant to dilute suspensions of axially symmetric microellipsoids irradiated by weak write beams whose wavelength is long compared to the particle dimensions. The latter ensures that the system is in the Rayleigh regime where scattering losses are small and the spatial variation of the electric field component of the write beams across the microparticle dimensions is negligible.

## II. PROBLEM FORMULATION

In this section we formulate the problem of the interaction of a shaped-microparticle suspension, maintained in either an electric field or an intense polarized radiation beam, with two degenerate write beams.<sup>18</sup> Section II A deals with the steady-state properties of the optical index gratings and their transient dynamics are discussed in Sec. II B.

### A. Electrodynamics of shaped-microparticle suspensions

We assume a monodisperse suspension of shaped microparticles characterized by a particle density  $n_0$  and a polarizability tensor  $\vec{\alpha}(\theta, \phi)$ ,

$$\vec{\alpha}(\theta, \phi) = \alpha_S \vec{\mathbf{I}} + \frac{1}{3} \beta \vec{\mathbf{K}}(\theta, \phi). \quad (2.1)$$

Here the angular variables  $(\theta, \phi)$  specify the orientation of the particle polarizability relative to a lab-fixed reference frame,  $\alpha_S(\beta)$  is the isotropic (anisotropic) component of the polarizability, and  $\vec{\mathbf{I}}$  [ $\vec{\mathbf{K}}(\theta, \phi)$ ] is the unit [orientation] tensor. The elements of the orientation tensor are

$$\vec{\mathbf{K}}(\theta, \phi) = \begin{pmatrix} 3 \sin^2 \theta \cos^2 \phi - 1 & 3 \sin^2 \theta \sin \phi \cos \phi & 3 \sin \theta \cos \theta \sin \phi \\ 3 \sin^2 \theta \sin \phi \cos \phi & 3 \sin^2 \theta \sin^2 \phi - 1 & 3 \sin \theta \cos \theta \cos \phi \\ 3 \sin \theta \cos \theta \sin \phi & 3 \sin \theta \cos \theta \cos \phi & 3 \cos^2 \theta - 1 \end{pmatrix}. \quad (2.2)$$

We suppose that the microparticle suspension is electromagnetically aligned and irradiated by two degenerate light beams that write a volume index grating. The orienting electric field is denoted by  $\mathbf{E}_S$ , while the vector sum of the two write beams, each oscillating at the frequency  $\omega$ , is denoted by  $\mathbf{E}_D(\mathbf{r}, t)$ . The host fluid is assumed to be passive and unaffected by both  $\mathbf{E}_S$  and  $\mathbf{E}_D(\mathbf{r}, t)$ . The particles are polarized by the applied fields and acquire a dipole moment  $\mathbf{p}(\theta, \phi; \mathbf{r}, t) = \vec{\alpha}(\theta, \phi) \cdot \mathbf{E}(\mathbf{r}, t)$ , where

$$\mathbf{p}(\theta, \phi; \mathbf{r}, t) = [\alpha_S \vec{\mathbf{I}} + \frac{1}{3} \beta \vec{\mathbf{K}}(\theta, \phi)] \cdot \mathbf{E}(\mathbf{r}, t) \quad (2.3)$$

and  $\mathbf{E}(\mathbf{r}, t) = \mathbf{E}_S + \mathbf{E}_D(\mathbf{r}, t)$ . The induced dipole will, in turn, couple back to the  $\mathbf{E}(\mathbf{r}, t)$  giving rise to a potential  $U(\theta, \phi; \mathbf{r}, t)$ , equal to

$$U(\theta, \phi; \mathbf{r}, t) = -\frac{1}{2} \langle \mathbf{E}(\mathbf{r}, t) \cdot \mathbf{p}(\mathbf{r}, t; \theta, \phi) \rangle_{\text{av}}, \quad (2.4)$$

where  $\langle \rangle_{\text{av}}$  implies a time average long compared to the optical period, but short compared to the medium response time  $\tau$ . If  $\omega\tau \gg 1$ , then there are two contributions:  $U(\theta, \phi; \mathbf{r}, t) = U_S(\theta, \phi) + U_D(\theta, \phi; \mathbf{r}, t)$ , with

$$U_j(\theta, \phi; \mathbf{r}, t) = -\frac{1}{2} \alpha_S \langle E_j^2 \rangle_{\text{av}} - \frac{1}{6} \beta \langle \mathbf{E}_j \cdot \mathbf{K}(\theta, \phi) \cdot \mathbf{E}_j \rangle_{\text{av}}. \quad (2.5)$$

This field-induced potential governs the microparticle distribution function  $n(\mathbf{r}; \theta, \phi)$ . In steady state,  $n(\mathbf{r}; \theta, \phi)$  is the Maxwell-Boltzmann distribution

$$n(\mathbf{r}; \theta, \phi) = n_0 \exp[-U(\mathbf{r}; \theta, \phi)/kT] / Z, \quad (2.6)$$

where  $Z$  is the partition function

$$Z = \int_0^L d\mathbf{r} \int_0^{2\pi} d\phi \int_0^\pi d\theta \sin \theta \exp \left[ -\frac{U(\mathbf{r}, \theta, \phi)}{kT} \right]. \quad (2.7)$$

The coupling between the microparticles and the write beams is assumed to be small compared to  $kT$ ; but their interaction with  $\mathbf{E}_S$  can be arbitrary. Thus  $U_S(\theta, \phi)/kT$  is of arbitrary size and since  $\xi \equiv U_D(\theta, \phi)/kT \ll 1$ , we may expand  $n(\mathbf{r}; \theta, \phi)$  in powers of  $\xi$ . Retaining terms up to first order in  $\xi$ , we have

$$n(\mathbf{r}; \theta, \phi) = n_S(\theta, \phi) [1 + \langle U_D(\mathbf{r}, \theta, \phi) / kT \rangle - U_D(\mathbf{r}, \theta, \phi) / kT]. \quad (2.8a)$$

The angular brackets imply an ensemble average over the distribution function

$$n_S(\theta, \phi) = \frac{n_0 \exp[-U_S(\theta, \phi) / kT]}{\int_0^L d\mathbf{r} \int_0^{2\pi} d\phi \int_0^\pi d\theta \sin\theta \exp\left[-\frac{U_S(\theta, \phi)}{kT}\right]}. \quad (2.8b)$$

The first term in Eq. (2.8a) is a spatially uniform, anisotropic distribution of microparticles whose orientational distribution is specified by the field-induced interaction  $U_S(\theta, \phi)$  and Brownian diffusion. The next two terms arise from and reflect the presence of the write beams that reorganize the spatial and orientational characteristics of the microparticle distribution.

Figure 1 depicts the situation of interest. The write beams are nearly collinear and their propagation direction specifies the  $z$  axis. The orienting field is taken to lie in the  $xy$  plane at an angle of  $\Phi$  with respect to the  $x$  axis, i.e.,  $\mathbf{E}_S = E_S(\mathbf{e}_x \cos\Phi + \mathbf{e}_y \sin\Phi)$  and

$$U_S(\theta, \phi) = g \sin^2\theta \cos^2(\theta - \Phi) - g/3, \quad (2.9)$$

where  $g = \beta E_S^2 / 2kT$ . If the orienting field is a polarized light beam of intensity  $I$ , then  $g = 4\pi\beta I / ckT$ .

As illustrative examples of required field strengths, we consider the two suspensions<sup>4,6</sup> used to achieve nonlinear optical processes. For an aqueous suspension of PTFE, where the low-frequency (200 kHz) polarizability  $\beta = 10^{-14} \text{ cm}^3$ , a value of  $g = 10$  requires an electric-field strength of 2.67 kV/cm. If a polarized light beam is used to align the particles, the dynamic polarizability enters into the problem and at argon-ion wavelength is equal to  $10^{-16} \text{ cm}^3$ . For a beam intensity of 1 MW/cm<sup>2</sup>,  $g = 10$ . For the carbon fiber suspension, the static polarizability

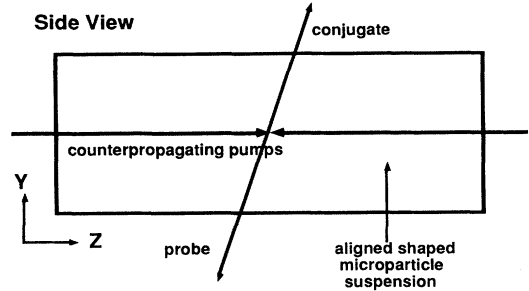
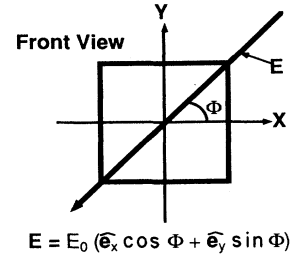


FIG. 1. Electromagnetically aligned, shaped-particle suspension maintained in an electric field and irradiated by two coherent light beams.

$\beta = 10^{-10} \text{ cm}^3$  and  $g = 10$  for an electric-field strength of 30 V/cm. If the particles are aligned with an 18-GHz beam, an intensity of 10 W/cm<sup>2</sup> will render  $g = 10$ .

The medium is irradiated by two degenerate coherent radiation beams:  $\mathbf{E}_D(\mathbf{r}, t) = \mathbf{E}_1(\mathbf{r}, t) + \mathbf{E}_2(\mathbf{r}, t)$ , where

$$\mathbf{E}_j(\mathbf{r}, t) = \frac{1}{2} E_{0j} [A_j(z, t) \mathbf{e}_x + B_j(z, t) \mathbf{e}_y] \times \exp[i(\mathbf{K}_j \cdot \mathbf{r} - \omega t)] + \text{c.c.}, \quad (2.10)$$

with  $E_{0j}$  and  $\mathbf{K}_j$  the initial amplitude and wave vector of the  $j$ th beam. The functions  $A_j(z, t)$  and  $B_j(z, t)$  specify the evolution of the two polarization components of the  $j$ th beam as it propagates through the shaped-microparticle suspension, and  $\mathbf{e}_x$  ( $\mathbf{e}_y$ ) is a unit vector in the  $x$  ( $y$ ) direction.

The interaction potential  $U_D^{(1,2)}(\mathbf{r})$  between the microparticles and both two write beams is, with  $\xi^{(1,2)}(\mathbf{r}, \theta, \phi) = U_D^{(1,2)}(\mathbf{r}) / kT$ ,

$$\begin{aligned} \xi^{(1,2)}(\mathbf{r}, \theta, \phi) = & \{g_T (A_1 A_2^* + B_1 B_2^*) + g_R [A_1 A_2^* K_{xx}(\theta, \phi) + B_1 B_2^* K_{yy}(\theta, \phi)] \\ & + (A_1 B_2^* + B_1 A_2^*) K_{xy}(\theta, \phi)\} \exp(i\mathbf{Q} \cdot \mathbf{r}) + \text{c.c.}, \end{aligned} \quad (2.11a)$$

with  $\mathbf{Q} \equiv \mathbf{K}_1 - \mathbf{K}_2$ ,  $g_T \equiv \alpha_S E_{01} E_{02} / 4kT$ ,  $g_R \equiv \beta E_{01} E_{02} / 12kT$ , and  $K_{jk} \equiv \mathbf{e}_j \cdot \mathbf{K} \cdot \mathbf{e}_k$ . The average inherent in  $\langle U_D(\mathbf{r}) \rangle$  ensures that only the self-interaction terms, i.e., the ones with  $j = k$ , are nonzero. These interactions usually give rise to self-focusing and nonlinear phase shifts, but they play no direct role in grating phenomena. Denoting this term by  $\mathcal{P}(\mathbf{r}, \theta, \phi)$ , we have

$$\mathcal{P}(\mathbf{r}, \theta, \phi) = g_T (I_1 + I_2) + g_R [ (|A_1|^2 + |A_2|^2) K_{xx}(\theta, \phi) + (|B_1|^2 + |B_2|^2) K_{yy}(\theta, \phi) + (A_1 B_1^* + B_2 A_2^*) K_{xy}(\theta, \phi) ], \quad (2.11b)$$

where  $I_j = (|A_j|^2 + |B_j|^2)$ .

For static index gratings, the portion of the microparticle distribution function of interest is

$$\delta n(\mathbf{r}, \theta, \phi) = -\xi^{(1,2)}(\mathbf{r}, \theta, \phi) n_S(\mathbf{r}, \theta, \phi). \quad (2.12)$$

The  $\mu\nu$  component of the optical index tensor grating,  $\delta\epsilon_{\mu\nu}(\mathbf{r}, \theta, \phi)$ , arising from these microparticle gratings, is given by

$$\begin{aligned} \delta\epsilon_{\mu\nu}(\mathbf{r}) &= \langle \alpha_{\mu\nu} \delta n(\mathbf{r}, \theta, \phi) \rangle \\ &= \langle (\alpha_S \delta_{\mu\nu} + \frac{1}{3} \beta K_{\mu\nu}) \delta n(\mathbf{r}, \theta, \phi) \rangle. \end{aligned} \quad (2.13)$$

Using Eq. (2.13), we have

$$\delta\epsilon_{\mu\nu}(\mathbf{r}) = \Delta\epsilon_{\mu\nu} \exp(i\mathbf{Q}\cdot\mathbf{r}) + \text{c.c.}, \quad (2.14a)$$

where  $\Delta\epsilon_{\mu\nu} = \Delta\epsilon_{\mu\nu}^{TT} + \Delta\epsilon_{\mu\nu}^R$  and

$$\Delta\epsilon_{\mu\nu}^{TT} = -g_T (A_1 A_2^* + B_1 B_2^*) \langle \alpha_{\mu\nu} \delta n(\mathbf{r}, \theta, \phi) \rangle, \quad (2.14b)$$

$$\begin{aligned} \Delta\epsilon_{\mu\nu}^R &= -\frac{1}{3} g_R \langle [(A_1 A_2^* K_{xx} + B_1 B_2^*) K_{yy} \\ &\quad + (A_1 B_2^* + B_1 A_2^*) K_{xy}] \alpha_{\mu\nu} n_S(\theta, \phi) \rangle. \end{aligned} \quad (2.14c)$$

This actually consists of four separate index gratings; each can coherently scatter radiation and enter into non-linear optical processes. Thus we set

$$\Delta\epsilon_{\mu\nu} = \sum_{P,Q} \Delta\epsilon_{\mu\nu}^{P,Q}, \quad (2.15)$$

where  $(P, Q)$  refer to the particle translational ( $T$ ) or rotational ( $R$ ) degrees of freedom:

$$\Delta\epsilon_{\mu\nu}^{R,T} = \beta g_T (A_1 A_2^* + B_1 B_2^*) \langle K_{\mu\nu}(\theta, \phi) n_S(\theta, \phi) \rangle, \quad (2.16a)$$

$$\begin{aligned} \Delta\epsilon_{\mu\nu}^{T,R} &= \alpha g_R \langle (A_1 A_2^* K_{xx} + B_1 B_2^* K_{yy} \\ &\quad + (A_1 B_2^* + B_1 A_2^*) K_{xy}) n_S(\theta, \phi) \rangle \delta_{\mu\nu}, \end{aligned} \quad (2.16b)$$

$$\begin{aligned} \Delta\epsilon_{\mu\nu}^{R,R} &= \beta g_R \langle K_{\mu\nu} [A_1 A_2^* K_{xx} + B_1 B_2^* K_{yy} \\ &\quad + (A_1 B_2^* + B_1 A_2^*) K_{xy}] n_S(\theta, \phi) \rangle. \end{aligned} \quad (2.16c)$$

An examination of these equations reveals that the particle index gratings consist of orientational averages of bilinear products of the polarizability tensor  $\langle \alpha_{\mu\nu} \alpha_{\delta\lambda} \rangle$  ensemble averaged over the distribution function  $n_S(\theta, \phi)$ . On physical grounds it is clear that the properties of these index gratings will depend intimately upon  $n_S(\theta, \phi)$ .

For our purposes it is convenient to introduce two sets of quantities:  $B_{\mu\nu\delta\lambda}(\theta, \phi)$  and  $\pi_{\mu\nu}^{P,Q}(\theta, \phi)$ . The first set is defined by the equation

$$B_{\mu\nu\delta\lambda}(\theta, \phi) = n_S(\theta, \phi) \alpha_{\mu\nu} \alpha_{\delta\lambda} \quad (2.17a)$$

and forms the basic constituents of the induced dipole moment density  $\pi_{\mu\nu}^{P,Q}(\theta, \phi)$ , defined by the equation

$$\langle \pi_{\mu\nu}^{P,Q}(\theta, \phi) \rangle = \Delta\epsilon_{\mu\nu}^{P,Q}. \quad (2.17b)$$

The physical content of  $\pi_{\mu\nu}^{P,Q}(\theta, \phi)$  can be appreciated by noting that the macroscopic nonlinear dipole moment  $P_{\mu;NL}(\mathbf{r}, t)$  for the suspension is given by

$$P_{\mu;NL} = \left[ \sum_{P,Q} \langle \pi_{\mu\nu}^{P,Q}(\theta, \phi) \rangle \exp(i\mathbf{Q}\cdot\mathbf{r}) + \text{c.c.} \right] E_\nu(\mathbf{r}, t). \quad (2.18)$$

## B. Transient dynamics of electromagnetically aligned shaped-microparticle suspensions

The transient dynamics of particle suspensions is governed by the Planck-Nernst equation for the distribution function. For a collection of identical, shaped microparticles maintained in a viscous fluid and subject to electromagnetic forces and torques, the Planck-Nernst equation is

$$\frac{\partial n}{\partial t} = D \left[ \nabla^2 n - \nabla \cdot \left[ \frac{\mathbf{F}}{kT} n \right] \right] - \Theta_0 \left[ L^2 n - \mathbf{L} \cdot \left[ \frac{\mathbf{\Gamma}}{kT} n \right] \right], \quad (2.19)$$

where  $\mathbf{L}$  is the microparticle angular momentum operator. Here  $D$  ( $\Theta_0$ ) is the particle diffusion coefficient for translational (orientational) motion. The field-induced forces are given by

$$\mathbf{F}(\mathbf{r}) = -\nabla U_D(\mathbf{r}, \theta, \phi), \quad (2.20a)$$

since a uniform electric field does not induce a force on the particles. The field-induced torques are

$$\mathbf{\Gamma}(\mathbf{r}) = -\mathbf{L} U_S(\mathbf{r}, \theta, \phi) - \mathbf{L} U_D(\mathbf{r}, \theta, \phi). \quad (2.20b)$$

The electrostrictive force  $\mathbf{F}(\mathbf{r})$  tends to drive particles into a translational grating that consists of periodic variations in the particle density. The time scale to create this translational grating is set by the response time  $\tau_D = 1/DQ^2$ , the time it takes for a microparticle to diffuse a distance  $1/Q$ . The values of  $D$  for suspensions used to generate phase-conjugate radiation<sup>10,12</sup> are  $10^{-7}$  cm<sup>2</sup>/sec for the PTFE suspension employed at argon-ion wavelengths and  $10^{-13}$  cm<sup>2</sup>/sec for the carbon fiber suspension used at 18 GHz. Thus the time to create a 10- $\mu$ m translational grating of shaped PTFE particles<sup>10,11</sup> is on the order of 1 sec, whereas the time to form a 1-cm translational grating in the shaped carbon fiber suspension is on the order of days. Since random, disruptive events are bound to occur on a much faster time scale, microwave radiation-induced density gratings will never manifest in the carbon fiber medium.

The shaped microparticles also experience electromagnetic torques: one arising from the uniform electric field and three different torques due to their interaction with the two write beams. Two of these torques are spatially uniform and do not give rise to microparticle index gratings. Thus they play no direct role in optical phase con-

jugation and can be ignored. The third torque arises from the simultaneous interaction of the microparticles with both write beams. This torque creates a spatially periodic, orientational grating that is responsible for generating phase conjugate light. The time scale for this grating to be set up depends upon the original orientational distribution. If the particles are initially unaligned, the time it takes to form an orientational index grating is set by the orientational diffusion time  $\tau_R \equiv 1/6\Theta_0$ . If, however, the microparticle distribution is initially anisotropic, then the time it takes to form an orientational grating will be reduced. Specifically, if the microparticles are initially restricted to lie within a narrow range of angles  $\delta\theta$ , about a direction specified by the orienting field, then the response time will be reduced by a factor of  $\delta\theta/\pi$ , and  $\delta\theta$  is proportional to  $1/g$ . For an aqueous suspension of PTFE microparticles, the orientational response time of an isotropic distribution is on the order of milliseconds,<sup>10,11</sup> whereas for the carbon fiber suspension it is on the order of 10 sec.<sup>12</sup> If the particles are initially prepared in an anisotropic state with  $g=10$ , then the grating formation time will be reduced by a factor of 10: to tenths of milliseconds and seconds, respectively.

From the discussion above, it follows that the orientational grating formation time is much shorter than the translational gratings formation time. Specifically,  $\tau_R/\tau_D \sim DQ^2/6\Theta_0 \sim 1/(Qa)^2$ , with  $a$  a typical particle dimension. On physical grounds, we anticipate that the formation time for orientational gratings should be on the order of  $(Qa)^2$  smaller than that of translational gratings. This reflects the fact that in order to create an orientational index grating, the microparticles must rotate through an angle of  $\pi$ , corresponding to diffusion over a distance  $\pi a$ . For translational gratings they must diffuse a distance of  $1/Q$ . Accordingly, the time scales over which translational and orientational grating phenomena occur will be quite different with the orientational grating forming well before the translational one. Thus the transient dynamics associated with the formation of these gratings can be examined within a Born-Oppenheimer type of approximation, in which the particle orientational grating adiabatically follows any changes in the translational grating.

For times  $t \ll \tau_D$ , we may ignore translational motion altogether and the Planck-Nernst equation can be simplified to

$$\frac{\partial n}{\partial t} + \Theta_0 L^2 n = -\Theta_0 \left[ \mathbf{L} \cdot \left[ n \frac{\mathbf{L}(U_L + U_S)}{kT} \right] \right]. \quad (2.21)$$

Since  $U_D \ll kT$ , it follows that the interaction between the microparticles and the write beams can be treated via perturbation theory. Thus setting

$$n(\mathbf{r}, t; \theta, \phi) = n_S(\mathbf{r}, t; \theta, \phi) + n_D(\mathbf{r}, t; \theta, \phi), \quad (2.22)$$

where  $n_S(\mathbf{r}, t; \theta, \phi)$  [ $n_D(\mathbf{r}, t; \theta, \phi)$ ] is the distribution function for the particles in  $E_S$  [first-order correction due to the write beams] and obeys

$$\frac{\partial n_S}{\partial t} + \Theta_0 L^2 n_S = -\Theta_0 \left[ \mathbf{L} \cdot \left[ n_S \frac{\mathbf{L}U_S}{kT} \right] \right], \quad (2.23a)$$

$$\begin{aligned} \frac{\partial n_D}{\partial t} + \Theta_0 L^2 n_D + \Theta_0 \left[ \mathbf{L} \cdot \left[ n_D \frac{\mathbf{L}U_S}{kT} \right] \right] \\ = -\Theta_0 \left[ \mathbf{L} \cdot \left[ n_S \frac{\mathbf{L}U_D}{kT} \right] \right], \end{aligned} \quad (2.23b)$$

for situations in which the microparticles are already in equilibrium with the orienting field, the governing equation for  $n_D(\mathbf{r}, t; \theta, \phi)$  is

$$\begin{aligned} \frac{\partial n_D}{\partial t} + \Theta_0 L^2 n_D + \Theta_0 \left[ \mathbf{L} \cdot \left[ n_D \frac{\mathbf{L}U_S}{kT} \right] \right] \\ = -\Theta_0 n_0 \left[ \mathbf{L} \frac{\exp[-U_S(\theta, \phi)/kT]}{Z_S} \cdot \left[ \frac{\mathbf{L}U_D}{kT} \right] \right]. \end{aligned} \quad (2.24)$$

### III. INDEX GRATINGS IN SHAPED-MICROPARTICLE SUSPENSIONS

In this section we examine the properties of electromagnetically aligned microparticle index grating and compare them to gratings formed in isotropic suspensions. The properties of the steady-state microparticle distribution and associated static index gratings of an unoriented suspension are reviewed in Sec. III A. In Sec. III B we investigate the steady-state attributes of aligned particle index gratings. Finally, in Sec. III C, the transient dynamics of grating formation and decay in an oriented suspension are discussed and contrasted with those exhibited by an isotropic particle suspension.

#### A. Unaligned shaped-microparticle index gratings

If a shaped-microparticle suspension is irradiated by weak light beams alone, i.e.,  $n_S(\theta, \phi) = n_0$ , then  $\pi_{\mu\nu}^{P,Q}(\theta, \phi)$  is given by

$$\Delta\pi(\theta, \phi)_{\mu\nu}^{T,T} = \alpha_S g_T (A_1 A_2^* + B_1 B_2^*) n_0 \delta_{\mu\nu}, \quad (3.1a)$$

$$\Delta\pi(\theta, \phi)_{\mu\nu}^{R,T} = \frac{1}{3} \beta g_T (A_1 A_2^* + B_1 B_2^*) K_{\mu\nu}(\theta, \phi) n_0, \quad (3.1b)$$

$$\begin{aligned} \Delta\pi(\theta, \phi)_{\mu\nu}^{T,R} = \alpha_S g_R [A_1 A_2^* K_{xx} + B_1 B_2^* K_{yy} \\ + (A_1 B_2^* + B_1 A_2^*) K_{xy}] n_0 \delta_{\mu\nu}, \end{aligned} \quad (3.1c)$$

$$\begin{aligned} \Delta\pi(\theta, \phi)_{\mu\nu}^{R,R} = \left(\frac{1}{3}\right)^2 \beta g_R K_{\mu\nu} [A_1 A_2^* K_{xx} + B_1 B_2^* K_{yy} \\ + (A_1 B_2^* + B_1 A_2^*) K_{xy}] n_0. \end{aligned} \quad (3.1d)$$

For an isotropic, microparticle suspension,

$$\langle K_{ij} \rangle = 0, \quad (3.2a)$$

$$\langle K_{jj}^2 \rangle = 16\pi/5, \quad \langle K_{ii} K_{jj} \rangle = -8\pi/5, \quad \langle K_{ij}^2 \rangle = 12\pi/5. \quad (3.2b)$$

The four optical index gratings reduce to

$$\epsilon_{\mu\nu}^{T,T} = \alpha_S g_T (A_1 A_2^* + B_1 + B_2^*) n_0 \delta_{\mu\nu}, \quad (3.3a)$$

$$\Delta\epsilon_{\mu\nu}^{R,T} = \Delta\epsilon_{\mu\nu}^{T,R} = 0, \quad (3.3b)$$

$$\Delta\epsilon_{xx}^{R,R} = (16\pi/5)\beta g_R (A_1 A_2^* - \frac{1}{2}B_1 B_2^*) n_0, \quad (3.3c)$$

$$\Delta\epsilon_{yy}^{R,R} = (16\pi/5)\beta g_R (B_1 B_2^* - \frac{1}{2}A_1 A_2^*) n_0, \quad (3.4a)$$

$$\Delta\epsilon_{xy}^{R,R} = \Delta\epsilon_{yx}^{R,R} = (12\pi/5)\beta g_R (A_1 B_2^* + B_1 A_2^*) n_0. \quad (3.4b)$$

All other matrix elements of the tensor  $\Delta\epsilon^{R,R}$  are zero. In the isotropic limit, it is straightforward to identify the origin of the different elements of the tensor set  $\Delta\epsilon_{\mu\nu}^{P,Q}$ . Thus the optical index grating whose amplitude is  $\Delta\epsilon_{\mu\nu}^{T,T}$  is clearly translational in nature and consists of a set of isotropic dipoles that are part of a microparticle density grating. Note that this grating is formed only if the two write beams have polarization components in the same direction. The last term  $\Delta\epsilon_{\mu\nu}^{R,R}$  is an orientational grating of anisotropic, polarizable microparticles whose optical characteristics are sensitive functions of the beam polarization and can be formed by beams that are polarized either parallel or orthogonal to one another.

The microparticle distribution is, to first-order in the write beams,

$$\begin{aligned} n(\mathbf{r}; \theta, \phi) = & n_0 + n_0 \{ g_T (A_1 A_2^* + B_1 B_2^*) \\ & + g_R [ A_1 A_2^* K_{xx}(\theta, \phi) + B_1 B_2^* K_{yy}(\theta, \phi) \\ & + (A_1 B_2^* + B_1 A_2^*) K_{xy}(\theta, \phi) ] \\ & \times \exp(i\mathbf{Q}\cdot\mathbf{r}) + \text{c.c.} \}. \end{aligned} \quad (3.5)$$

The terms that are proportional to  $g_T$  give rise to the translational grating and have no orientational preference, whereas those that are proportional to  $g_R$  give rise to the orientational grating and tend to point in a direction specified by the write beams. As an illustrative example, consider the case in which the two write beams are plane polarized in the same direction. For this case,  $A_1 = A_2 = 1$  and  $B_1 = B_2 = 0$ ,

$$n(\mathbf{r}; \theta, \phi) = n_0 + n_0 [ g_T + g_R (\sin^2 \theta \cos^2 \phi - \frac{1}{3}) ] \cos \mathbf{Q}\cdot\mathbf{r}, \quad (3.6a)$$

and we have taken the two write beams to be in phase for simplicity. For beams of equal intensity

$$\begin{aligned} n(\mathbf{r}; \theta, \phi) = & n_0(\theta, \phi) [ 1 + g_T \cos \mathbf{Q}\cdot\mathbf{r} \\ & + g_R (\sin^2 \theta \cos^2 \phi - \frac{1}{3}) (1 + \cos \mathbf{Q}\cdot\mathbf{r}) ]. \end{aligned} \quad (3.6b)$$

The angular dependence of the first two grating spacings in the plane  $\phi=0$  for the case  $g_T=0$ ,  $g_R=0.4$  is illustrated<sup>19</sup> in Fig. 2. An examination of this figure reveals that the microparticles tend to be oriented in the direction  $\theta=\pi/2$ , i.e., the particle distribution is anisotropic in the plane defined by the equation  $\mathbf{Q}\cdot\mathbf{r}=2n\pi$ . It is unaligned, i.e., the microparticle distribution is isotropic in the plane defined by the equation  $\mathbf{Q}\cdot\mathbf{r}=(2n+1)\pi$ . Be-

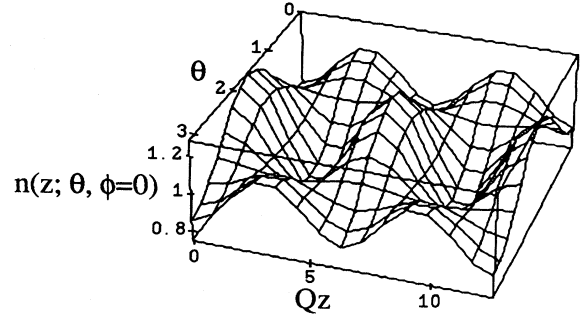


FIG. 2. Angular dependence of microparticle density over two grating spacings.

tween these planes, the microparticles tend to be aligned, although to a lesser extent. Thus as one scans along the grating direction, the particle distribution alternates periodically from being isotropic, at the points where the beams interfere destructively and the particles are not coupled to the interference pattern formed by the two write beams, to being anisotropic where the beams interfere constructively and the interaction between the microparticles and the radiation interference pattern is most intense.

The macroscopic dipole moment densities for this case are

$$\pi(\theta, \phi)_{\mu\nu}^{T,T} = \alpha_S g_T n_0 \delta_{\mu\nu}, \quad (3.7a)$$

$$\pi(\theta, \phi)_{\mu\nu}^{R,T} = \frac{1}{3} \beta g_T K_{\mu\nu}(\theta, \phi) n_0, \quad (3.7b)$$

$$\pi(\theta, \phi)_{\mu\nu}^{T,R} = \frac{1}{3} \alpha_S g_R K_{xx} n_0 \delta_{\mu\nu}, \quad (3.7c)$$

$$\pi(\theta, \phi)_{\mu\nu}^{R,R} = (\frac{1}{3})^2 \beta g_R K_{\mu\nu} K_{xx} n_0. \quad (3.7d)$$

In Fig. 3, we have depicted the  $\theta$  dependence of the different dipole moment densities in the plane  $\phi=0$  with  $\beta=\alpha_S$ . An examination of this figure reveals that all of

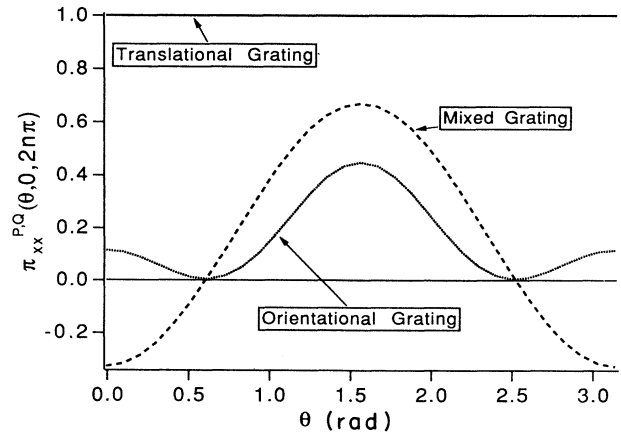


FIG. 3. Dipole moment densities for a shaped-microparticle suspension irradiated by two degenerate coherent beams. The microparticle suspension is such that  $\beta=\alpha_S$ .

the  $\pi(\theta, \phi)_{\mu\nu}^{P,Q}$  are symmetrical about  $\theta = \pi/2$ . Also the mixed gratings are degenerate and are as often negative as positive. Thus the mixed gratings average to zero and only the pure translational and rotational dipole moment densities will contribute to the nonlinear dipole moment of the suspension. In particular,

$$\epsilon_{\mu\nu}^{T,T} = \alpha_S g_T n_0 \delta_{\mu\nu}, \quad (3.8a)$$

$$\Delta \epsilon_{\mu\nu}^{R,T} = \Delta \epsilon_{\mu\nu}^{T,R} = 0, \quad (3.8b)$$

$$\Delta \epsilon_{xx}^{R,R} = (16\pi/5) \beta g_R n_0, \quad (3.8c)$$

$$\Delta \epsilon_{yy}^{R,R} = (8\pi/5) \beta g_R n_0, \quad (3.8d)$$

$$\Delta \epsilon_{xy}^{R,R} = 0. \quad (3.8e)$$

A static electric field will tend to alter the dipole moment densities as well as the optical index gratings  $\Delta \epsilon_{\mu\nu}^{P,Q}$  of the suspension. In particular, the mixed gratings  $\epsilon_{\mu\nu}^{T,R}$  and  $\epsilon_{\mu\nu}^{R,T}$  will no longer vanish.

### B. Electromagnetically aligned microparticle index gratings

The microparticle distribution and dipole moment densities are examined in Sec. III B 1 and the index gratings in Sec. III B 2 for an electromagnetically aligned, shaped-particle suspension that is irradiated by two write beams. For the case considered here, we assume that the static dielectric function of the microparticles is larger than that of the host fluid. This implies that  $g > 0$  for microrods and  $g < 0$  for microdisks. A similar assumption is made regarding the index of refraction of the fluid and the particles at the frequency of the write beams.

#### 1. Distribution functions and dipole moment densities

As an illustrative example we consider the case of two-plane parallel polarized write beams. The microparticle distribution  $n(\mathbf{r}, \theta, \phi)$  is

$$n(\mathbf{r}, \theta, \phi) = n_S(\theta, \phi) + n_S(\theta, \phi) [g_T + \frac{1}{3} g_R K_{xx}(\theta, \phi)] \cos \mathbf{Q} \cdot \mathbf{r}. \quad (3.9)$$

In Fig. 4, we have depicted the  $\theta$  dependence of the first two grating spacings for an electromagnetically aligned suspension of microrods with  $g = 10$ . Note that the distribution is much more sharply defined with the microparticles confined to point in the direction  $\theta = \pi/2$ . A more detailed view of this can be obtained by viewing the angular dependence of the distribution function in the plane  $z = 0$ . In the absence of an electric field, the distribution function is weakly peaked in the direction  $\theta = \pi/2$ . In the presence of an electric field the particle distributions become more oriented in the direction  $\theta = \pi/2$ . The rms width of the distribution  $\langle (\delta\theta)^2 \rangle^{1/2}$  is of order  $1/g$ , for large values of  $g$ , reflecting the role of  $n_S(\theta, \phi)$  in the structure of the index grating. The distribution function for rods is depicted below in Fig. 5 for the cases  $g = 2, 5$ , and  $10$ .

These highly anisotropic microparticle distributions

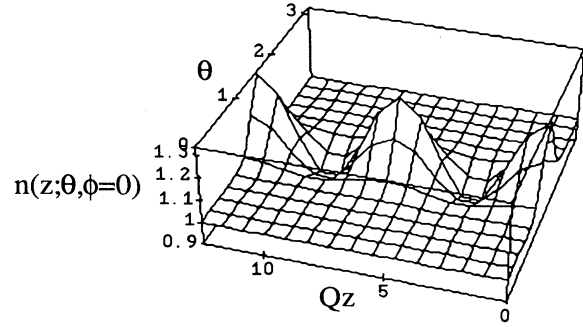


FIG. 4. Depicts the first two grating spacings of the microparticle distribution in the plane  $\phi = 0$ . For the case depicted, the microrods are electromagnetically aligned with  $g = 10$ .

have different electrodynamic characteristics; for example, they all have a net static dipole moment and the fact that the particles are aligned in a particular direction will enhance their dynamic dipole moments as well. This last feature of microparticle electrostatics can be appreciated by examining the angular dependence of the dipole moment densities. In particular, see Fig. 6, which depicts the dipole moment densities for the translational, mixed, and orientational gratings. In this figure, the write beams are plane polarized in the  $x$  direction and  $g = 10$ . An examination of this figure indicates that in the presence of a strong orienting field, the mixed gratings will no longer vanish (in this write beam polarization they are equal) since the dipole moment densities  $\pi_{xx}^{R,T}$  and  $\pi_{xx}^{T,R}$  are positive over the angular range of interest.

In Fig. 7, we have depicted the  $\theta$  dependence of the first two grating spacings for an electromagnetically aligned suspension of microdiscs with  $g = -10$ . Note that the distribution is much more sharply defined with the microparticles confined to point in the direction  $\theta = 0$  and  $\pi$ . A more detailed view of this can be obtained by viewing the angular dependence of the distribution func-

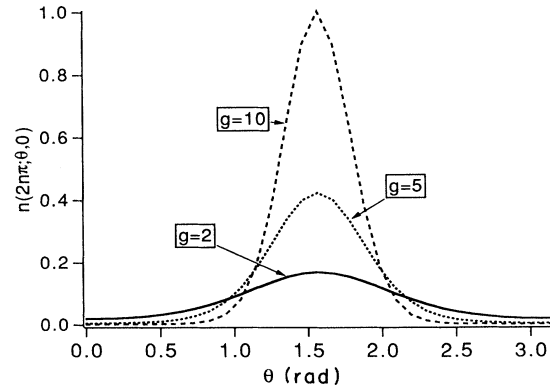


FIG. 5. Depicts the  $\theta$  dependence, of the microrod distribution in the plane  $\phi = 0$  and  $\mathbf{Q} \cdot \mathbf{r} = 2n\pi$ , for the case  $g_T = 0.2$ ,  $g_R = 0.2$  with the orienting field parallel to the  $x$ -axis and parallel polarized write beams with  $g = 2, 5, 10$ . The microparticle suspension is such that  $\beta = \alpha_S$ . The distribution is normalized so that its maximum value is unity.

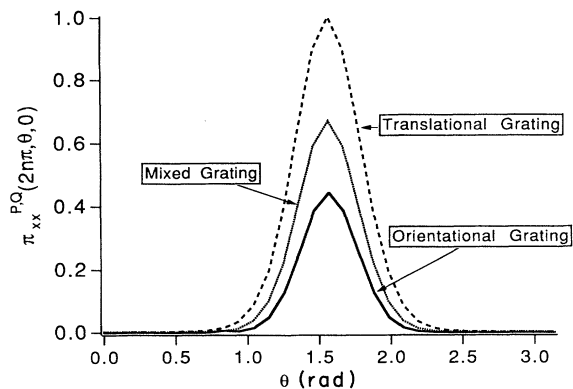


FIG. 6. Dipole moment density associated with the translational, mixed, and orientational gratings for a suspension of microrods maintained in an orienting field with  $g=10$ . The write beams are both plane polarized in the  $x$  direction. The densities are normalized so that the maximum value of the translational grating is unity.

tion in the plane  $z=0$  for a variety of values of  $g$ . This is done in Fig. 8, which depicts the  $\theta$  dependence of the microparticle distribution for a collection of microdisks in an orienting field that is parallel to the  $x$  axis. The cases  $g=-2, -5$ , and  $-10$  are depicted. The figure depicts a point where the beams interfere coherently, i.e.,  $\mathbf{Q} \cdot \mathbf{r} = 2n\pi$ . An examination of this figure reveals that the presence of an electric field greatly alters the angular dependence of the distribution function. Specifically, the microdisk orientation becomes increasingly localized in the directions  $\theta=0$  and  $\pi$ .

Figure 9 depicts the dipole moment densities for the translational, mixed, and orientational gratings of a suspension of disk-shaped microparticles that are electromagnetically aligned by an orienting field. In this figure, the write beams are plane polarized in the  $x$  direction and  $g=-10$ . An examination of this figure indicates that in the presence of a strong orienting field, the mixed gratings will no longer vanish (in this write beam polarization they are equal) since the dipole moment densities  $\pi_{xx}^{R,T}$  and  $\pi_{xx}^{T,R}$  are positive over the angular range of interest.

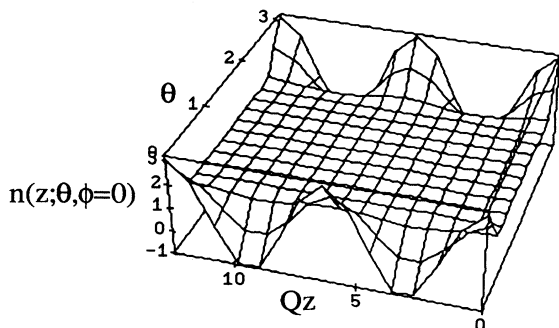


FIG. 7. Depicts the first two grating spacings of the microparticle distribution in the plane  $\phi=0$ . For the case depicted, the microdisks are electromagnetically aligned with  $g=-10$ .

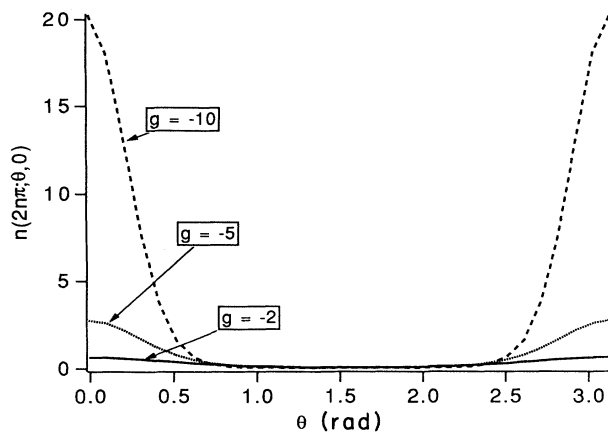


FIG. 8. Depicts the  $\theta$  dependence of the microdisk distribution in the plane  $\phi=0$  and  $\mathbf{Q} \cdot \mathbf{r} = 2n\pi$ , for the case  $g_T=0.2$ ,  $g_R=-0.2$  with the orienting field parallel to the  $x$  axis and parallel polarized write beams with  $g=-2, -5, -10$ . The microparticle suspension is such that  $\beta=\alpha_S$ .

## 2. Grating depth

In this section, we examine the role of the field strength and orientation of  $\mathbf{E}_S$  in modifying the properties of the microparticle optical index gratings. Specifically, we study the dependence on  $g$  and  $\Phi$  of the grating matrix elements  $\langle K_{ij} \rangle$  and  $\langle K_{ij} K_{lm} \rangle$ . The properties of the original orientational grating matrix elements  $\langle K_{xx}^2 \rangle$ ,  $\langle K_{xy}^2 \rangle$ , and  $\langle K_{xx} K_{yy} \rangle$  are examined first. We then discuss the translational-orientational gratings  $\langle K_{xx} \rangle$  and  $\langle K_{xy} \rangle$  and finally the new orientational grating  $\langle K_{xx} K_{xy} \rangle$ . To ease the comparison to the zero-field limit, all grating matrix elements are normalized with respect to  $\langle K_{xx}^2(0) \rangle$ , the largest zero-field matrix element.

Figure 10 depicts the dependence of  $\langle K_{xx}^2(g) \rangle / \langle K_{xx}^2(0) \rangle$  on  $g$  for a microparticle suspension

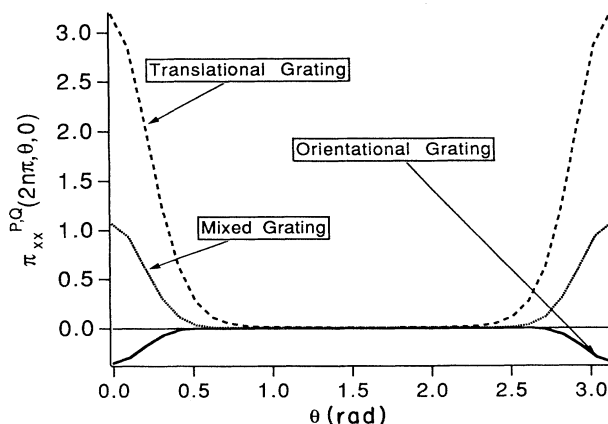


FIG. 9. Dipole moment densities for a suspension of microdisks maintained in an orienting field with  $g=-10$ . The write beams are both plane polarized in the  $x$  direction.



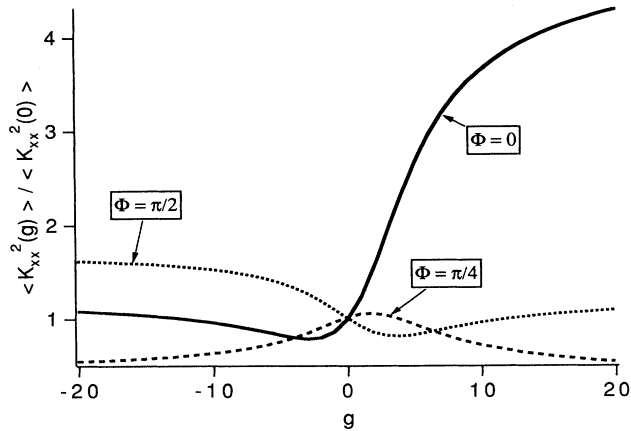


FIG. 10. Depicts the  $g$  dependence for  $\langle K_{xx}^2(g) \rangle / \langle K_{xx}^2(0) \rangle$  with the field oriented at  $0^\circ$ ,  $45^\circ$ , and  $90^\circ$  with respect to the  $x$  axis.

maintained in an electric field that is oriented at the angles  $\Phi = 0^\circ$ ,  $45^\circ$ , and  $90^\circ$  with respect to the  $x$  axis. This quantity controls four-wave mixing processes in which both the read and write beams are plane polarized in the  $x$  direction. An examination of this figure reveals that aligning the particles can significantly enhance the grating depth. For example, if  $\mathbf{E}_S$  is parallel to the  $x$  axis, the matrix element for microrods will saturate at a value that is six times larger than its zero-field value. This corresponds to the situation in which all of the particles are aligned parallel to the electric field ( $\theta = \pi/2$  and  $\phi = 0$ ). For disk-shaped particles, this matrix element exhibits a complex dependence on the electric field strength as  $\mathbf{E}_S$  initially aligns the microparticles normal to the direction mandated by the write beams in order to create an optical index grating. This initially decreases the grating depth and is a clear manifestation of the different behavior that rods and disks display when the suspension is electromagnetically aligned. Eventually, the grating depth saturates to a value slightly greater than its zero-field value.

If the field is aligned at  $45^\circ$  with respect to the  $x$  axis, the grating depth is, in general, smaller than the zero-field value because  $\mathbf{E}_S$  and the write beams tend to align the microparticles in different directions. This tends to reduce the grating depth, which eventually falls to about 31% of its zero field value. Note that microrods and microdisks behave in roughly the same way for this field configuration. If the electric field points in the  $y$  direction, then it tends to align the microrods normal to the direction mandated by the write beams so that the grating depth is initially reduced. The converse is true for disks and  $\langle K_{xx}^2(g) \rangle / \langle K_{xx}^2(0) \rangle$  increases with the application of an orienting field. Finally,  $\langle K_{yy}^2(g) \rangle / \langle K_{xx}^2(0) \rangle$  exhibits exactly the same behavior as  $\langle K_{xx}^2(g) \rangle / \langle K_{xx}^2(0) \rangle$ , provided  $\Phi \rightarrow \Phi - \pi/2$ .

Next we examine the index grating  $\langle K_{xy}^2(g) \rangle / \langle K_{xx}^2(0) \rangle$ , which plays the dominant role in four-wave mixing processes where the write beams are plane polarized orthogonal to one another with the pumps polarized parallel to one another. Three field

orientations are considered:  $\Phi = 0^\circ$ ,  $45^\circ$ , and  $90^\circ$  with respect to the  $x$  axis. An examination of Fig. 11 reveals that  $\langle K_{xy}^2(g) \rangle / \langle K_{xx}^2(0) \rangle$  is maximized if  $\mathbf{E}_S$  is directed at an angle of  $45^\circ$  with respect to the  $x$  axis, as is expected on physical grounds. More precisely, the write beams tend to align the particles at an angle of  $45^\circ$  with respect to the  $x$  axis, so that aligning  $\mathbf{E}_S$  in the same direction gives rise to the maximum possible enhancement of the grating depth for rod-shaped microparticles. For disk-shaped particles,  $\mathbf{E}_S$  aligns the particles normal to the direction preferred by the write beams and this tends to reduce the grating depth. For situations in which the electric field is oriented in the  $x$  or  $y$  direction,  $\langle K_{xy}^2(g) \rangle / \langle K_{xx}^2(0) \rangle$  is in general reduced because the field tends to align the particles in a direction different from that preferred by the write beams. In general, rod-shaped microparticles tend to have deeper gratings than disk-shaped ones.

The last of the original orientational gratings involved in optical phase conjugation is  $\langle K_{xx}(g)K_{yy}(g) \rangle / \langle K_{xx}^2(0) \rangle$ . This microparticle index grating dominates four-wave mixing processes in which the write beams are polarized parallel to each other, but the pump beams are orthogonally polarized to one another. Figure 12 depicts the dependence of this matrix element on the parameter  $g$  for three different field orientations:  $0^\circ$ ,  $45^\circ$ , and  $90^\circ$ . An examination of this figure reveals that the matrix element is enhanced only if the electric field is oriented at an angle of  $45^\circ$  with respect to the  $x$  axis, a feature due to the fact that the system is symmetric about  $\Phi = 45^\circ$ . Note the strong asymmetry between microrods and microdisks.

Next we examine the new optical index gratings that have both translational and orientational attributes:  $\Delta\epsilon_{\mu\nu}^{T,R}$  and  $\Delta\epsilon_{\mu\nu}^{R,T}$ . These index gratings are mixed in the sense that they are formed on an orientational time scale; however, as can be seen from Eq. (2.13), they involve  $\alpha_S$ , the isotropic polarizability, which is associated with the existence of translational gratings in optical phase conjugation. More precisely, we study the normalized matrix

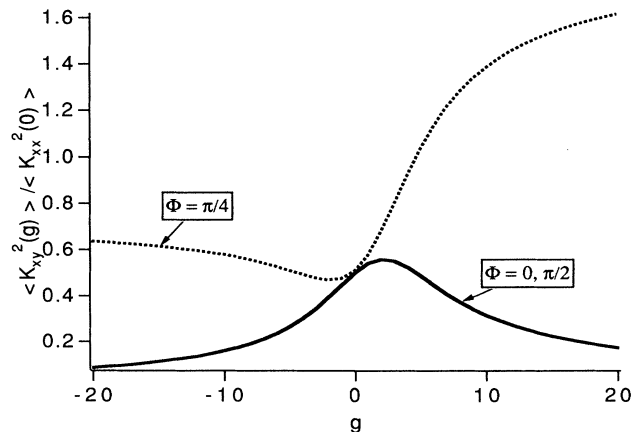


FIG. 11. Depicts the  $g$  dependence for  $\langle K_{xy}^2(g) \rangle / \langle K_{xx}^2(0) \rangle$  with the field oriented at  $0^\circ$ ,  $45^\circ$ , and  $90^\circ$  with respect to the  $x$  axis.

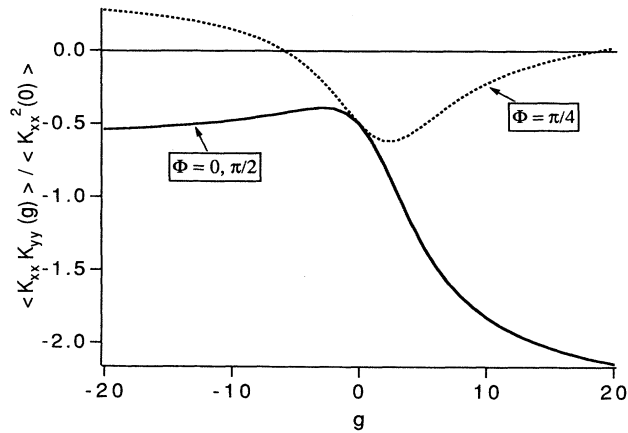


FIG. 12. Depicts the  $g$  dependence for  $\langle K_{xx}(g)K_{yy}(g) \rangle / \langle K_{xx}^2(0) \rangle$  with the field oriented at  $0^\circ$ ,  $45^\circ$ , and  $90^\circ$  with respect to the  $x$  axis.

elements  $\langle K_{xx}(g) \rangle / \langle K_{xx}^2(0) \rangle$  and  $\langle K_{xy}(g) \rangle / \langle K_{xx}^2(0) \rangle$ . In linear optics,  $\langle K_{xx}(g) \rangle$  and  $\langle K_{yy}(g) \rangle$  are associated with electric-field-induced phase shifting, birefringence, and polarization modulation. In the absence of  $E_S$ ,  $\langle K_{xx}(g) \rangle$  and  $\langle K_{yy}(g) \rangle$  vanish as they require an anisotropic medium to be nonzero. Figure 13 depicts  $\langle K_{xx}(g) \rangle / \langle K_{xx}^2(0) \rangle$  versus  $g$  for the three field orientations:  $\Phi = 0^\circ$ ,  $45^\circ$ , and  $90^\circ$ . An examination of this figure reveals that the grating depth is a maximum if  $E_S$  is oriented parallel to the  $x$  axis. Note that for this field configuration, the grating saturates to a maximum value of 2 as  $g \rightarrow \infty$ , corresponding to the situation in which all of the microrods are aligned parallel to the electric field. For disks, the microparticles align perpendicular to the field and the grating depth saturates to the value  $-1$ . Thus, for disk-shaped microparticles, this new grating is out of phase with respect to the pure orientational and translational gratings:  $\Delta\epsilon_{\mu\nu}^{T,T}$  and  $\Delta\epsilon_{\mu\nu}^{R,R}$ . This is a new feature of aligned microparticle electrodynamics and

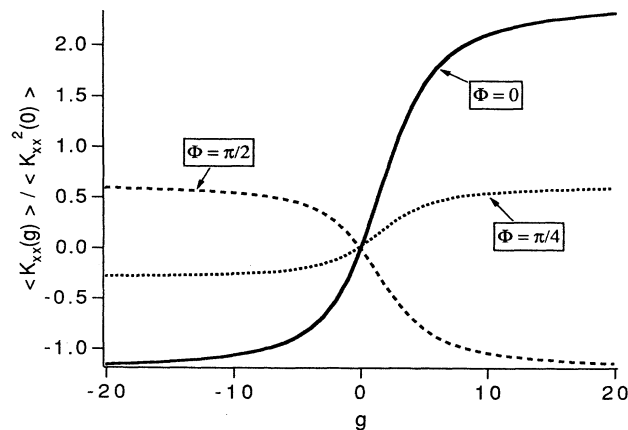


FIG. 13. Depicts the  $g$  dependence for  $\langle K_{xx}(g) \rangle / \langle K_{xx}^2(0) \rangle$  with the field oriented at  $0^\circ$ ,  $45^\circ$ , and  $90^\circ$  with respect to the  $x$  axis.

manifests itself by reducing the magnitude of the phase-conjugate reflectivity. Note, too, that if the field is oriented in the  $y$  direction, the phase of the grating is reversed with respect to  $0^\circ$  and the grating depth saturates to the value of  $-1$ , corresponding to the microrods being aligned perpendicular to the direction preferred by the radiation beams. This feature gives rise to a reduction of the phase-conjugate reflectivity and has already been observed experimentally.<sup>17</sup> For disk-shaped particles, they tend to be oriented perpendicular to  $E_S$  as  $g \rightarrow -\infty$ ; however, they are in phase with  $\Delta\epsilon_{\mu\nu}^{T,T}$  and  $\Delta\epsilon_{\mu\nu}^{R,R}$ .

Figure 14 depicts the dependence of the microparticle index grating  $\langle K_{xy}(g) \rangle / \langle K_{xx}^2(0) \rangle$  on  $g$  for the same orientations. An examination of this figure reveals that the grating depth is a maximum if the electric is oriented at  $45^\circ$  with respect to the  $x$  axis. Note that the index grating does not form if the field is oriented in either the  $x$  or  $y$  directions, due to symmetry. At  $45^\circ$ , the grating depth saturates at the value of 2 for rod-shaped particles and  $-1$  for disk-shaped microparticles.

Finally, we examine the index gratings  $\langle K_{xx}(g)K_{xy}(g) \rangle / \langle K_{xx}^2(0) \rangle$  and  $\langle K_{yy}(g)K_{xy}(g) \rangle / \langle K_{xx}^2(0) \rangle$ , which do not appear unless the symmetry of the suspension is greatly reduced by an electric field that is appropriately oriented. Physically, these gratings arise in four-wave-mixing processes in which both the read and write beams are linearly polarized in the same direction, but the emitted conjugate wave has a component polarized perpendicular to the input waves. The microparticle index  $\langle K_{xx}(g)K_{xy}(g) \rangle / \langle K_{xx}^2(0) \rangle$  is depicted in Fig. 15. An examination of this figure reveals that the matrix element is zero if the electric field or polarized light beam is oriented parallel to either the  $x$  or  $y$  axis and is a maximum at  $45^\circ$ , due to symmetry, where it saturates to a value of 0.8 for rods and 0.2 for disks. Symmetry demands that  $\langle K_{yy}(g)K_{xy}(g) \rangle / \langle K_{xx}^2(0) \rangle$  be the same as  $\langle K_{xx}(g)K_{xy}(g) \rangle / \langle K_{xx}^2(0) \rangle$  provided  $\Phi \rightarrow \Phi - \pi/2$ .

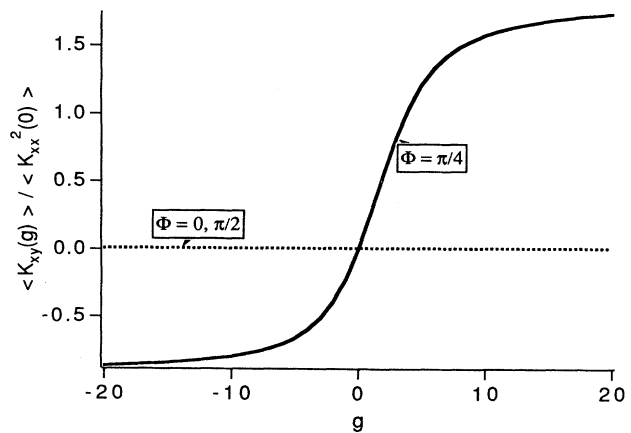


FIG. 14. Depicts the  $g$  dependence for  $\langle K_{xy}(g) \rangle / \langle K_{xx}^2(0) \rangle$  with the field oriented at  $0^\circ$ ,  $45^\circ$ , and  $90^\circ$  with respect to the  $x$  axis.

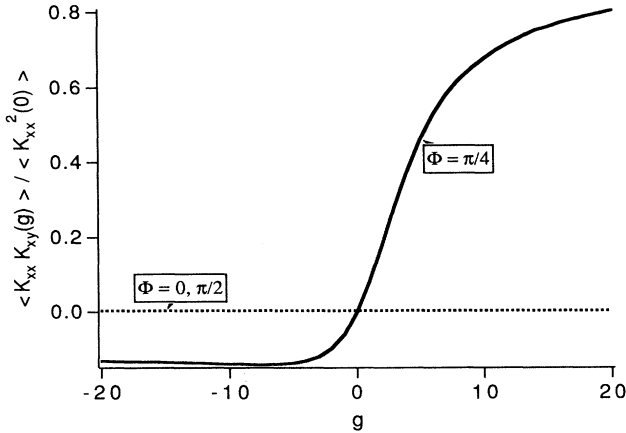


FIG. 15. Depicts the  $g$  dependence for  $\langle K_{xx}(g)K_{xy}(g) \rangle / \langle K_{xx}^2(0) \rangle$  with the field oriented at  $0^\circ$ ,  $45^\circ$ , and  $90^\circ$  with respect to the  $x$  axis.

### C. Transient dynamics of aligned microparticle index gratings

The transient dynamics of aligned, radiation-induced particle index gratings is examined in this section. The influence of an orienting field on the grating formation and decay times is determined. In addition, the time required for the suspension to evolve from one ordered state to another is examined.

The medium response time is set by the angular range ( $\delta\theta$ ) that the microparticles must rotate divided by their angular velocity. If the suspension is maintained in an intense orienting field, i.e.,  $g \gg 1$ , then the microparticles will be constrained to point within a narrow range of angles about the direction specified by the orienting field. Thus  $\delta\theta$  is reduced from its zero field value of  $\pi$  to  $\pi/g$  and the medium response times are reduced by the same amount.

To determine the transient dynamics of the orientational gratings created within the microparticle suspension, we examine the evolution of the nonlinear polarization

$$\begin{aligned} \mathbf{P}_{\text{NL}}(\mathbf{r}, t) &= \langle \vec{\alpha} \delta n(\mathbf{r}, t) \rangle \cdot \mathbf{E}(\mathbf{r}, t) \\ &= \alpha_S \langle \delta n(\mathbf{r}, t) \rangle \mathbf{E}(\mathbf{r}, t) + \frac{1}{3} \beta \langle \delta n(\mathbf{r}, t) \vec{\mathbf{K}} \rangle \cdot \mathbf{E}(\mathbf{r}, t). \end{aligned} \quad (3.10)$$

The time evolution of the translational-orientational gratings  $\langle K_{xx} \rangle$  and  $\langle K_{xy} \rangle$  is determined by  $\langle \delta n(\mathbf{r}, t) \rangle$  and the different orientational gratings by  $\langle \delta n(\mathbf{r}, t) \vec{\mathbf{K}} \rangle$ .

Figure 16 depicts the transient behavior of the  $\langle K_{xx} \rangle$  ( $\parallel$ ) and  $\langle K_{xy} \rangle$  ( $\perp$ ) microparticle index gratings for  $g=5$  with the field oriented at an angle of  $45^\circ$  with respect to the  $x$  axis. An examination of this figure reveals that the response times for the  $\langle K_{xx} \rangle$  grating are about twice as fast as those of  $\langle K_{xy} \rangle$ . Note that the microparticles response time is somewhat reduced by the presence of a Stark field as these gratings achieve their steady-state values at times of  $1.5\tau_R$  ( $\parallel$ ) and  $3\tau_R$  ( $\perp$ ). After the index

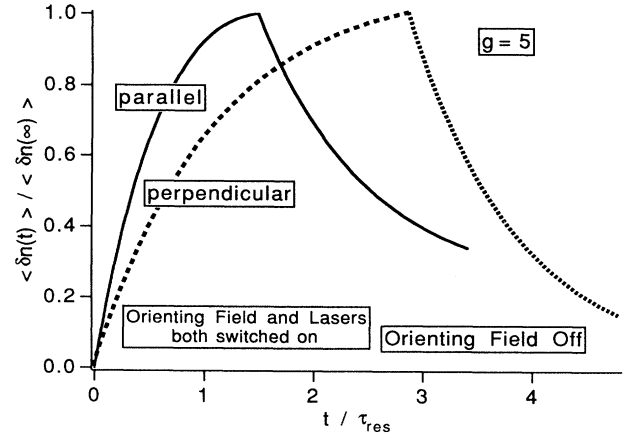


FIG. 16. Depicts the transient behavior of the orientational index gratings  $\langle K_{xx} \rangle$  and  $\langle K_{xy} \rangle$  for  $g=5$  and the electric field oriented at an angle of  $45^\circ$  with respect to the  $x$  axis.

gratings achieve their steady-state values, the orienting field is switched off and the gratings decay to zero, their steady-state value for  $g=0$ . As the decay time is over twice the formation time, it is clear that the torque arising from the interaction of the shaped particles with either an applied electric field or polarized light beam does affect the suspension's response time.

Next we examine the formation time of the orientational index gratings. In particular, we study the transient dynamics of the matrix elements  $\langle \delta n(\mathbf{r}, t) K_{xx} \rangle$  and  $\langle \delta n(\mathbf{r}, t) K_{xy} \rangle$ . For the first grating, the write beams are assumed to be linearly polarized in the same direction; so that as  $t \rightarrow \infty$ , the grating evolves to the steady-state value of  $\langle K_{xx}^2(g) \rangle$ . For the second grating the write beams are assumed to be linearly polarized in the orthogonal directions; so that as  $t \rightarrow \infty$ , the grating evolves towards the steady-state value of  $\langle K_{xy}^2(g) \rangle$ . These are responsible for the formation of the optical index gratings  $\Delta \epsilon_{xx}^{R,R}$  and  $\Delta \epsilon_{xy}^{R,R}$ .

Figure (17) depicts these quantities for the cases  $g=5$

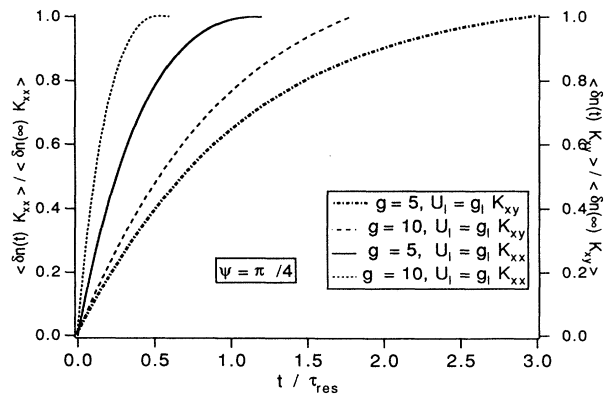


FIG. 17. Formation of the orientational gratings  $\langle K_{xx}^2(t) \rangle$  and  $\langle K_{xy}^2(t) \rangle$  for  $g=5$  and  $10$ , with the electric field oriented at  $45^\circ$  with respect to the  $x$  axis.

and 10, with the electric field at an angle of  $45^\circ$  with respect to the  $x$  axis. Note that the grating formed by the parallel-polarized beams has the shorter response time, despite the fact that  $\Phi=45^\circ$ . An examination of this figure reveals that the response time for the  $\langle K_{xx}^2 \rangle$  grating is on the order of  $(1/2g)$  of its value in the absence of an electric field. Note that the  $\langle K_{xy}^2 \rangle$  grating formation time is longer, being reduced by a factor of  $(5/g)$ .

The importance of  $\Phi$  can be seen from Fig. 18, which depicts the formation time for the normalized matrix element  $\langle K_{xx}^2(g) \rangle / \langle K_{xx}^2(0) \rangle$  for the electric field pointing at the three angles:  $\Phi=0$ ,  $\pi/4$ , and  $\pi/2$ , with  $g=5$ . An examination of this figure reveals that the grating formation time is most reduced if the applied electric field is parallel to the polarization of the writing beams and it is slowest if it is perpendicular to the write beams. In particular, if the field is parallel to the  $x$  axis, the microparticles are 63% oriented by  $t=0.2\tau_{\text{Res}}$ , whereas if the field is oriented in the  $y$  direction, the microparticles are 63% oriented by  $t=0.8\tau_{\text{Res}}$ . Thus the orientation of the electric field relative to the polarization direction can influence the grating formation time by a factor of 4.

It is also of interest to examine the transient dynamics of these index gratings as the microparticle suspension evolves from one state to another. Specifically, we study the transition of a microparticle grating from the state in which an orienting field is present to one in which the field is turned off, but the write beams are still on. This corresponds to a switch from one type of microparticle grating to another. Specifically, in an oriented suspension all the microparticles tend to be aligned in a direction specified by the orienting field, and superimposed on this is the particle index grating that consists of a periodic tightening and easing of the microparticle alignment about the preferred angle. In an isotropic suspension the gratings consist of periodic, alternating regions in which the particles are aligned and then unaligned. The degree and direction of alignment of these microparticle index

gratings is determined by the write beams. Figure 19 depicts the transient evolution of the suspension as it evolves from the first state to the second.

#### IV. DISCUSSION AND CONCLUSIONS

In this paper we examined the optical and dynamical properties of index gratings created by two degenerate, phase coherent write beams in an aligned, shaped-microparticle suspension. The microparticles can be aligned by means of electrostrictive torques generated by the interaction of the microparticle anisotropic polarizability with either an electric field or intense polarized radiation. This aligned suspension is anisotropic in nature and exhibits very different index grating characteristics from those of an isotropic suspension. These differences are summarized below.

Four novel effects are predicted to occur: (i) A scattering mechanism appears that gives rise to the formation of optical index gratings. (ii) With the exception of the translational grating the depth of all the other index gratings is strongly affected by the magnitude and orientation of the Stark field. For some situations the orientational gratings are measurably enhanced, while for others they are reduced. (iii) The degeneracy between rods and disks is split in the sense that the optical characteristics of their gratings are quite different even if the physical parameters are the same, as occurs in the field's absence. (iv) The formation and decay times of these microparticle index gratings are reduced.

These effects arise from and reflect the fact that an electric field will tend to restrict the microparticles to within a relatively narrow range of angles. This restriction in microparticle orientation alters the macroscopic properties of the suspension in a number of striking ways. For example, in the presence of an electric field, grating formation requires that the microparticles rotate through much smaller angles than in its absence. Accordingly, a static electric field will reduce grating response times in shaped-microparticle suspensions. Furthermore, as the particle orientation is confined to within a small range of

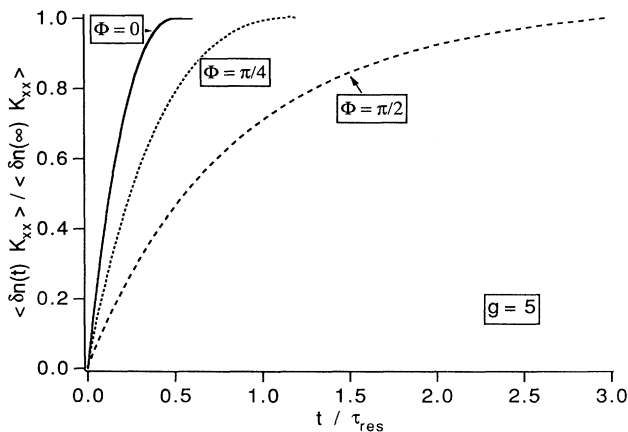


FIG. 18. Formation of the orientational gratings  $\langle K_{xx}^2(t) \rangle$  for  $g=5$  with the electric field oriented at  $0^\circ$ ,  $45^\circ$ , and  $90^\circ$  with respect to the  $x$  axis. The fastest response time occurs when the field is parallel to the  $x$  axis.

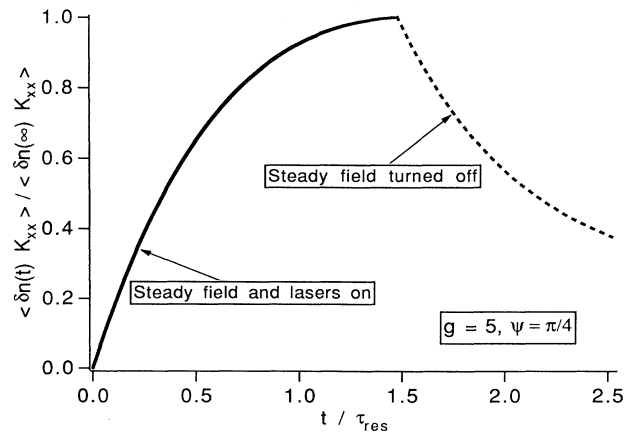


FIG. 19. Transient evolution from an aligned microparticle index grating to an unaligned index grating.

angles about a direction, determined by the electric field, their individual dipole moments will tend to be in phase and add coherently. This should be contrasted to the situation in which only weak radiation fields are present. For this case, the microparticle distribution is nearly isotropic, so that most of the particles are randomly aligned, giving rise to a much smaller net induced dipole moment than that displayed by a highly oriented suspension. This strong anisotropy in the microparticle orientation gives rise to a new scattering mechanism that alters the magnitude of the original effect. In addition, the phase of some of the new index gratings depends upon the direction of the electric field relative to the beam polarization. Thus these new gratings can be either in or out of phase with respect to the original orientational gratings and this will be reflected in the medium's four-wave mixing coefficients. Finally, the potential minima for disks and rods differ not only in angle, but also in magnitude. This aspect of the physics of shaped-particle suspensions manifests itself in the medium's electrostatics when the particle distribution becomes noticeably anisotropic.

Next we discuss the possible extension of these concepts to other active media that form orientational index gratings as a mechanism for realizing nonlinear optical processes. We consider two additional classes of orientational media: molecular rotators and liquid crystals in the isotropic phase.

Molecular rotators such as carbon disulfide or nitrobenzene generally have additional mechanisms for achieving index gratings and our comments are confined to the orientational gratings alone. On physical grounds, we anticipate that the concepts discussed in this paper for shaped-microparticle suspensions are applicable to heavy, symmetrical molecular rotators. This view is underscored by the fact that the polarizability of molecular rotators is described in the same way as for a shaped microparticle. For small molecules, such as  $H_2$ , quantization of the molecule's rotational degrees of freedom will somewhat alter the nature of the effect of an orienting field on the induced optical index. However, for heavier systems such as carbon disulfide, quantization of the molecular degrees of freedom should be unimportant and the general statements made here about microparticles should extend to molecular rotators. As shown in this paper, particle alignment becomes important for values of the dimensionless parameter  $g$  on the order of unity and dominates for  $g$  on the order of five. For molecular rotators, the anisotropy coefficient is on the order of  $10^{-19}$ – $10^{-21}$  cm<sup>3</sup>. To attain  $g = 1$  at room temperature, we require electric field strengths of  $(2.67 \times 10^5)$ – $(2.67 \times 10^6)$  V/cm. Such field strengths are beyond the breakdown voltage. However, observable effects should be possible with sufficiently intense laser

fields. Thus, for  $g = 1$ , the required laser intensity  $I = ckT/4\pi\beta$ , which varies from 0.1–10 GW/cm<sup>2</sup>. Such power is available with pulsed lasers. A 10-mJ, 10-nsec Nd:YAG (where YAG represents yttrium aluminum garnet) laser pulse, focused down to 100  $\mu$ m, provides laser intensities on the order of 3 GW/cm<sup>2</sup>. This should be adequate to alter the original molecular orientational gratings and to create new ones, provided that the medium response time is fast enough. For CS<sub>2</sub>, the medium response time is picoseconds and for nitrobenzene it is nanoseconds, so detection of the effect should be possible. With respect to response time, we note that molecular rotators do not obey the Planck-Nernst equation, which describes the dynamics of the microparticles as they rotate and translate in a viscous fluid. Simple molecular rotators obey the Debye relaxation equation, which is similar to the Planck-Nernst equation but not identical. Thus some differences between the dynamics of these two systems will arise.

Asymmetric molecular rotators are another interesting and possibly important class of nonlinear media that might be used as a means to achieve Stark-aligned optical index gratings. These materials are often endowed with sizable, permanent electric dipole moments that might be used to orient the molecules more readily, which can be achieved with the molecular polarizability. For example, such materials as tobacco mosaic virus have large static dipole moments ( $\mu$ ) on the order of  $10^4$  D. For this case,  $g = \mu E/kT$  and values of  $g$  on the order of unity can be achieved with electric-field strengths of 300 V/cm. We note that asymmetric rotators cannot be described with the polarizability used in Eq. (2.1) and the theory must be reformulated for the more general case of an asymmetric rotator.

Liquid crystals in the isotropic phase are another potential system of interest. In this phase, they do not interact strongly with one another and if they are symmetric will have the same electrostatics as shaped microparticles. However, since their physical dimensions are on the order of 100–1000 Å, their anisotropic polarizabilities will be on the order of  $10^{-16}$ – $10^{-18}$  cm<sup>3</sup>. This implies electric-field strengths on the order of  $10^4$ – $10^5$  V/cm or laser intensities of 30–300 MW/cm<sup>2</sup> to achieve values of  $g$  on the order of unity.

In this paper, we examined the effect of preparing a shaped-microparticle suspension in an anisotropic state on the properties of its optically induced orientational gratings. By placing the system in an oriented state, the optical and dynamical properties of these index gratings are altered. The altered gratings will give rise to modified nonlinear optical characteristics in such processes as optical phase conjugation. In future papers we will examine the nonlinear optics of oriented media.

<sup>1</sup>A. J. Palmer, *Opt. Lett.* **5**, 54 (1980).

<sup>2</sup>P. W. Smith, P. J. Maloney, and A. Ashkin, *Opt. Lett.* **7**, 347 (1982); A. Ashkin, J. M. Dziedzic, and P. W. Smith, *ibid.* **7**, 276 (1982).

<sup>3</sup>D. Rogovin, *Phys. Rev. A* **31**, 2375 (1985).

<sup>4</sup>B. Bobbs, R. Shih, H. Fetterman, and W. Ho, *Appl. Phys. Lett.* **52**, 4 (1988).

<sup>5</sup>R. McGraw, D. Rogovin, W. Ho, B. Bobbs, R. Shih, and H.

- Fetterman, Phys. Rev. Lett. **61**, 943 (1988).
- <sup>6</sup>R. Pizzoferrato, M. Marinelli, U. Zammit, F. Scudieri, S. Martellucci, and M. Romanagnoli, Opt. Commun. **68**, 231 (1988).
- <sup>7</sup>R. Piazza, J. Stavens, T. Belleni, and V. DeGiorgio, Opt. Commun. **73**, 263 (1989).
- <sup>8</sup>T. Belleni, R. Piazza, C. Sozzi, and V. DeGiorgio, Europhys. Lett. **7**, 561 (1988).
- <sup>9</sup>D. Rogovin, Opt. News **15**, 14 (1989).
- <sup>10</sup>M. De Spirito, R. Pizzoferrato, U. Zammit, M. Marinelli, F. Scudieri, and M. Romagnoli, Opt. Lett. **14**, 1356 (1989).
- <sup>11</sup>R. Pizzoferrato, M. De Spirito, U. Zammit, M. Marinelli, F. Scudieri, and S. Martellucci, Phys. Rev. A **41**, 2882 (1990).
- <sup>12</sup>R. Shih, H. Fetterman, W. Ho, R. McGraw, and B. Bobbs, Phys. Rev. Lett. **65**, 579 (1990).
- <sup>13</sup>R. Pizzoferrato, D. Rogovin, and J. Scholl, Opt. Lett. **16**, 297 (1991).
- <sup>14</sup>S. Sari and D. Rogovin, Opt. Lett. **9**, 414 (1984).
- <sup>15</sup>D. Rogovin, Phys. Rev. A **32**, 2837 (1985).
- <sup>16</sup>D. Rogovin, Phys. Rev. Lett. **65**, 567 (1990).
- <sup>17</sup>R. Pizzoferrato (private communication).
- <sup>18</sup>The write beams are at a different frequency than the aligning beam.
- <sup>19</sup>It is possible to prepare a water-glycerol PTFE suspension that has  $\alpha_S$  equal to zero, but  $\beta$  nonzero. This was done in Ref. 10.